

# CBC Parameter Estimation

GW Open Data Workshop #7, 2024

Soichiro Morisaki

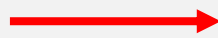
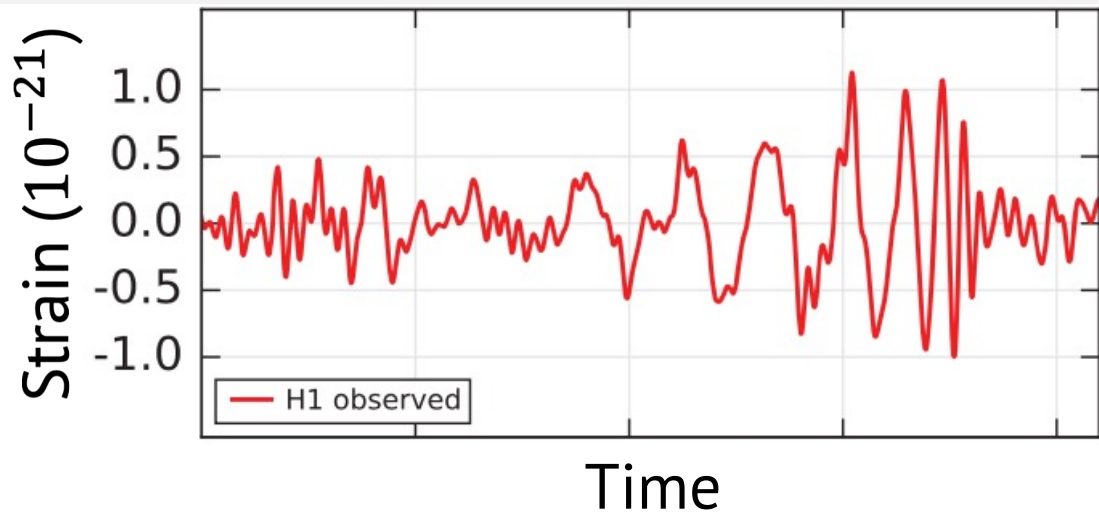


THE UNIVERSITY OF TOKYO

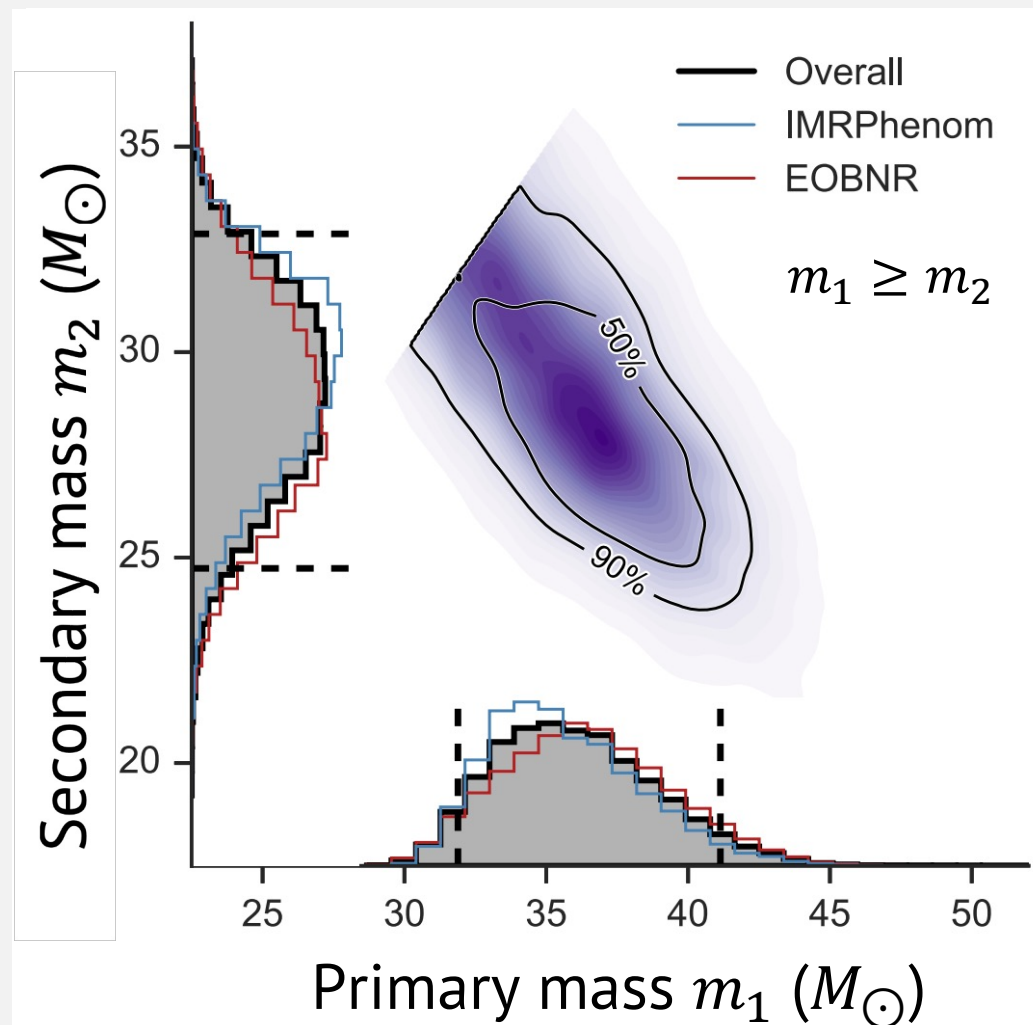


# Source Characterization from Data

Credit:  
B. P. Abbott et al., PRL **116**, no.6, 061102 (2016).



Credit: B. P. Abbott et al., PRL **116**, no.6, 241102 (2016).



# Masses: $m_1, m_2$

Higher masses  
→ Shorter and louder signal

Chirp mass  $\mathcal{M}$  is measured most precisely,

$$\mathcal{M} = \frac{(m_1 m_2)^{\frac{3}{5}}}{(m_1 + m_2)^{\frac{1}{5}}}$$

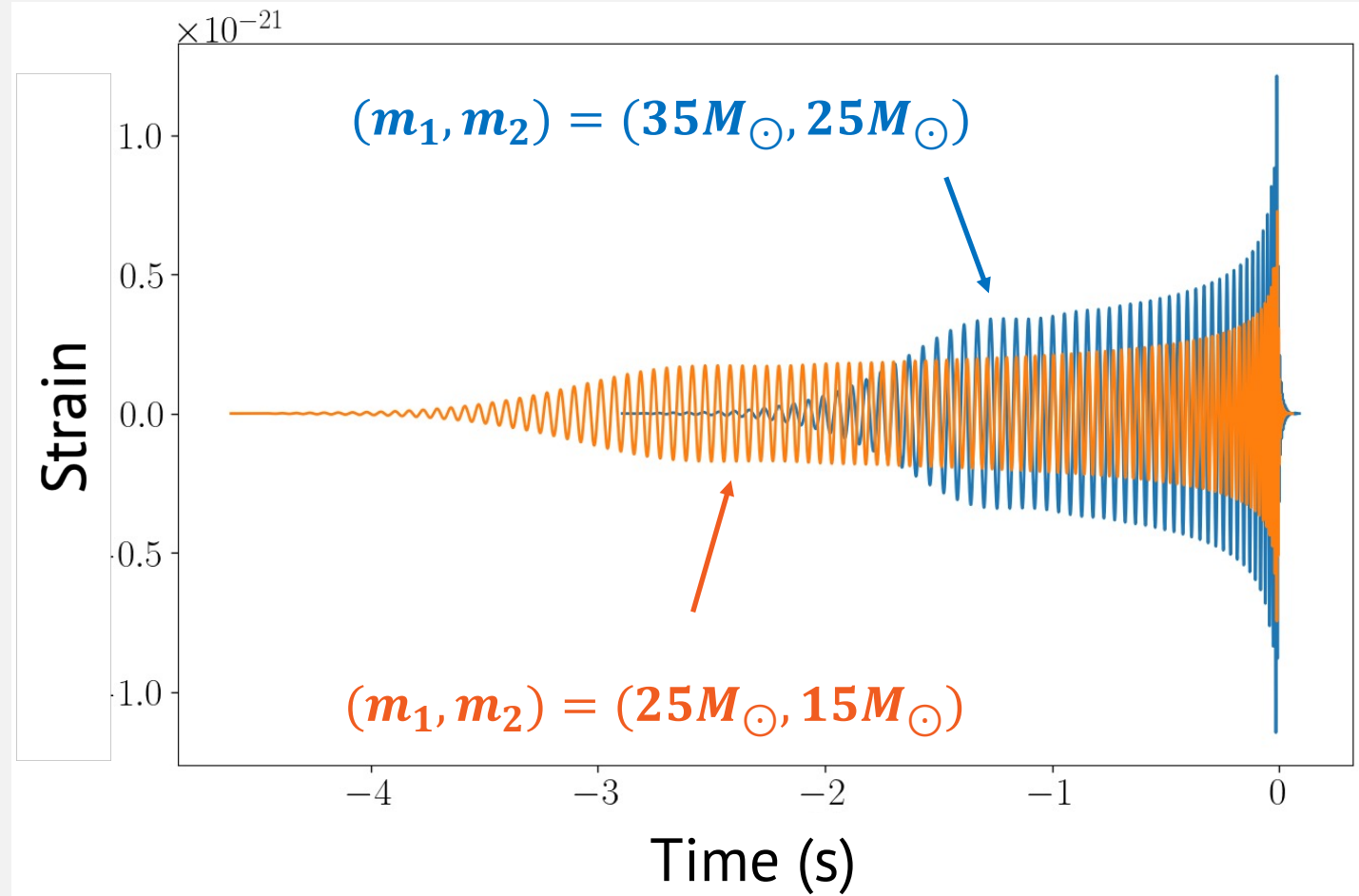
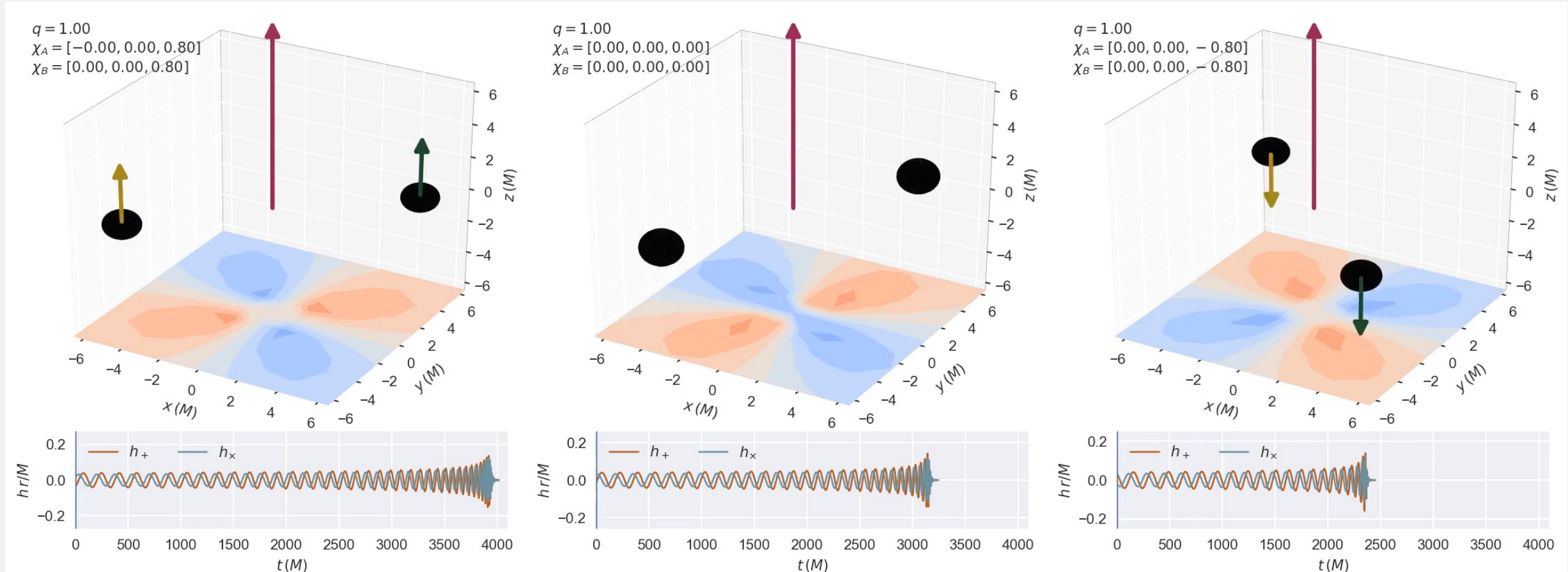


Figure: CBC signals starting from 20Hz

# Spins: $\vec{\chi}_1, \vec{\chi}_2$

Spins aligned with orbital angular momentum  $\rightarrow$  longer signal



Credit: Vijay Varma et al., Binary Black Hole Explorer

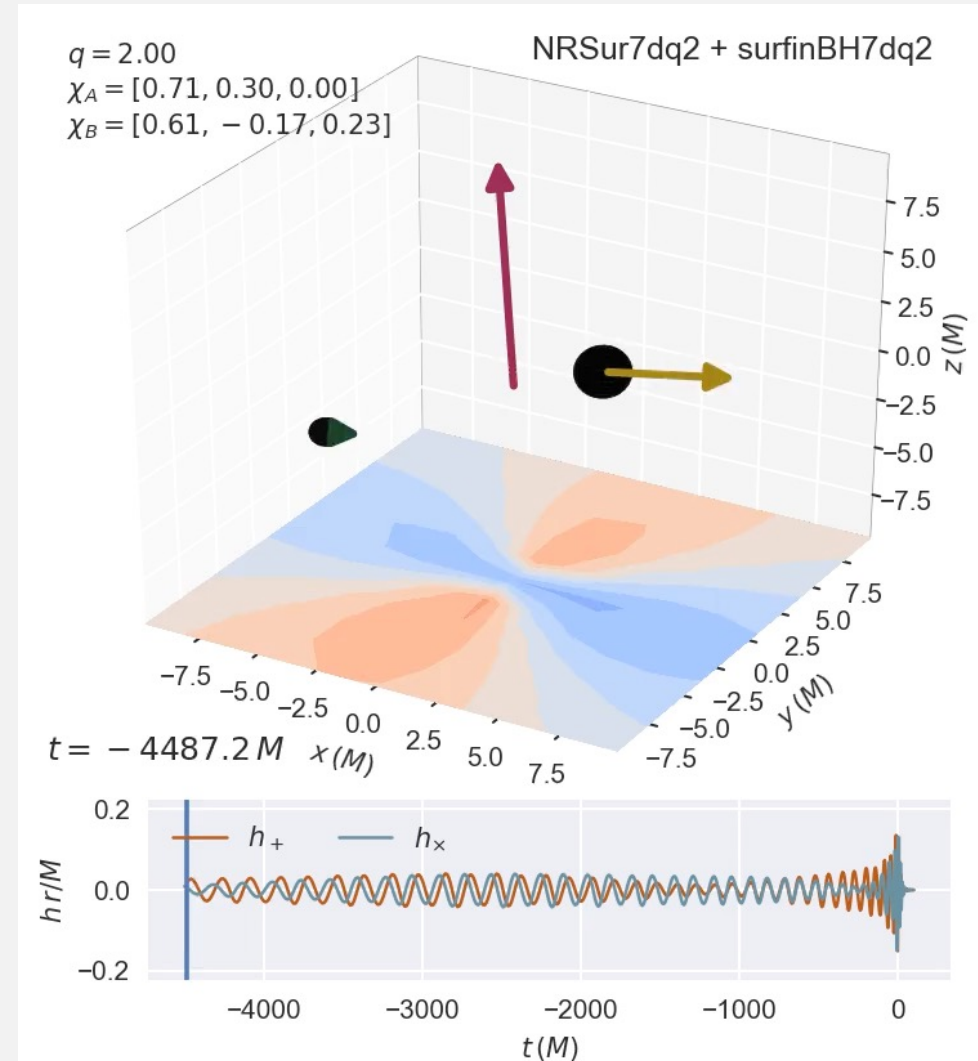
# Spins: $\vec{\chi}_1, \vec{\chi}_2$

Orthogonal spin components

→ Precession of orbital plane

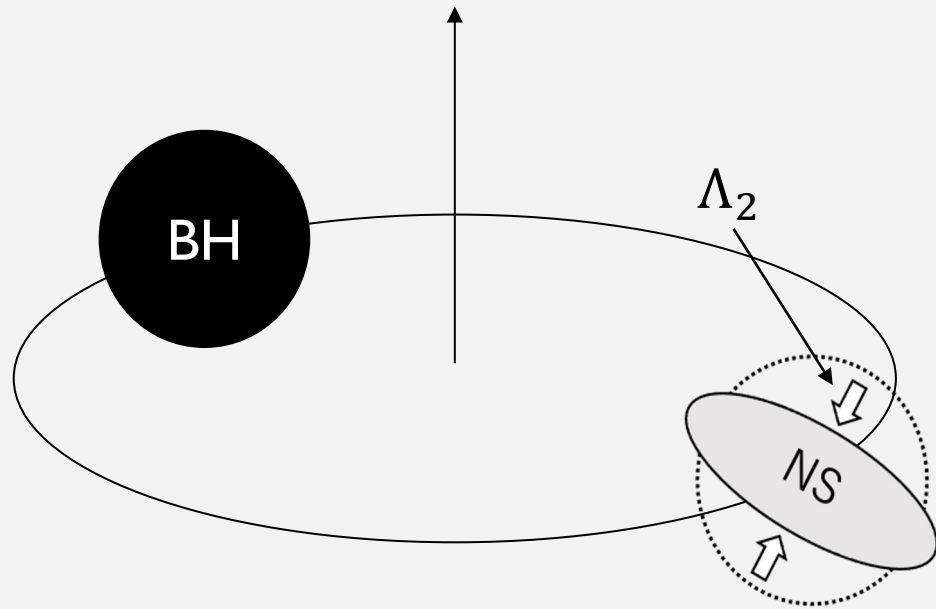
→ Amplitude and phase modulation

Masses and spins are key to probe the formation history of merging binary black holes.

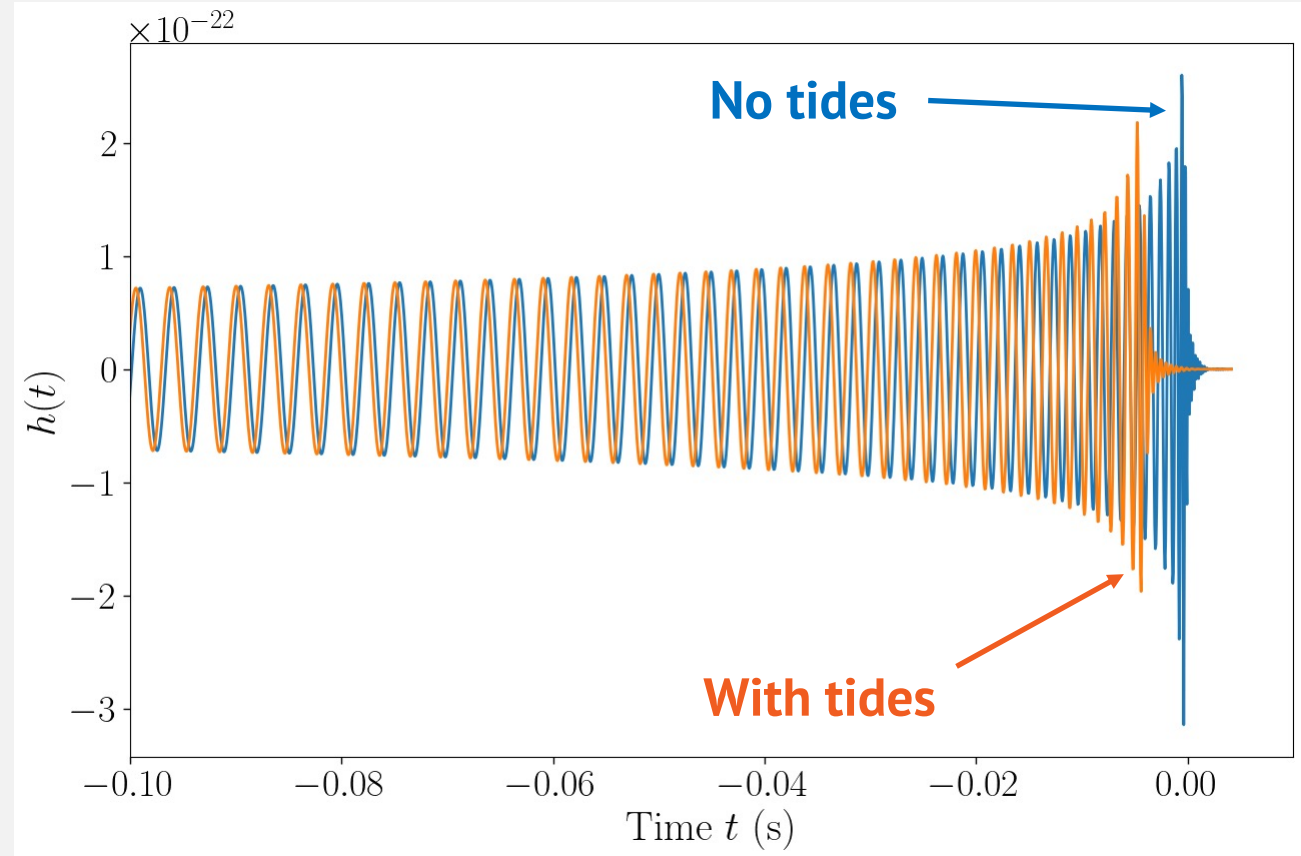


# Tidal deformability parameters: $\Lambda_1, \Lambda_2$

Tidal deformation of star  
accelerates orbital motion.

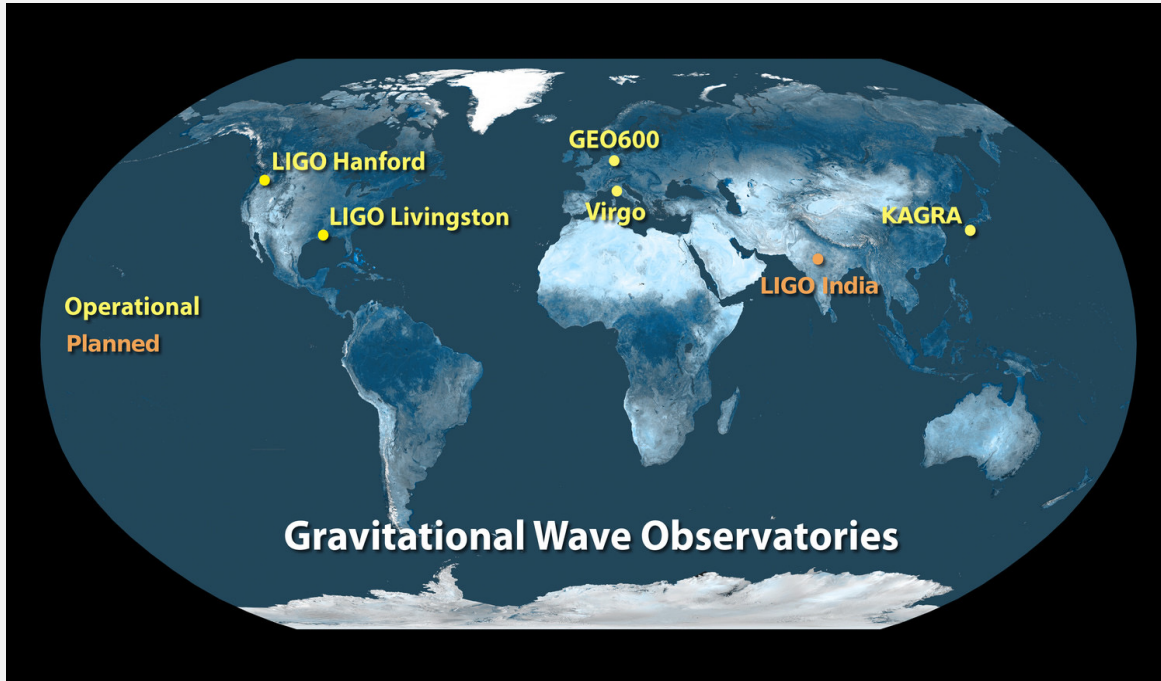


Can constrain the properties of  
highly dense matter.

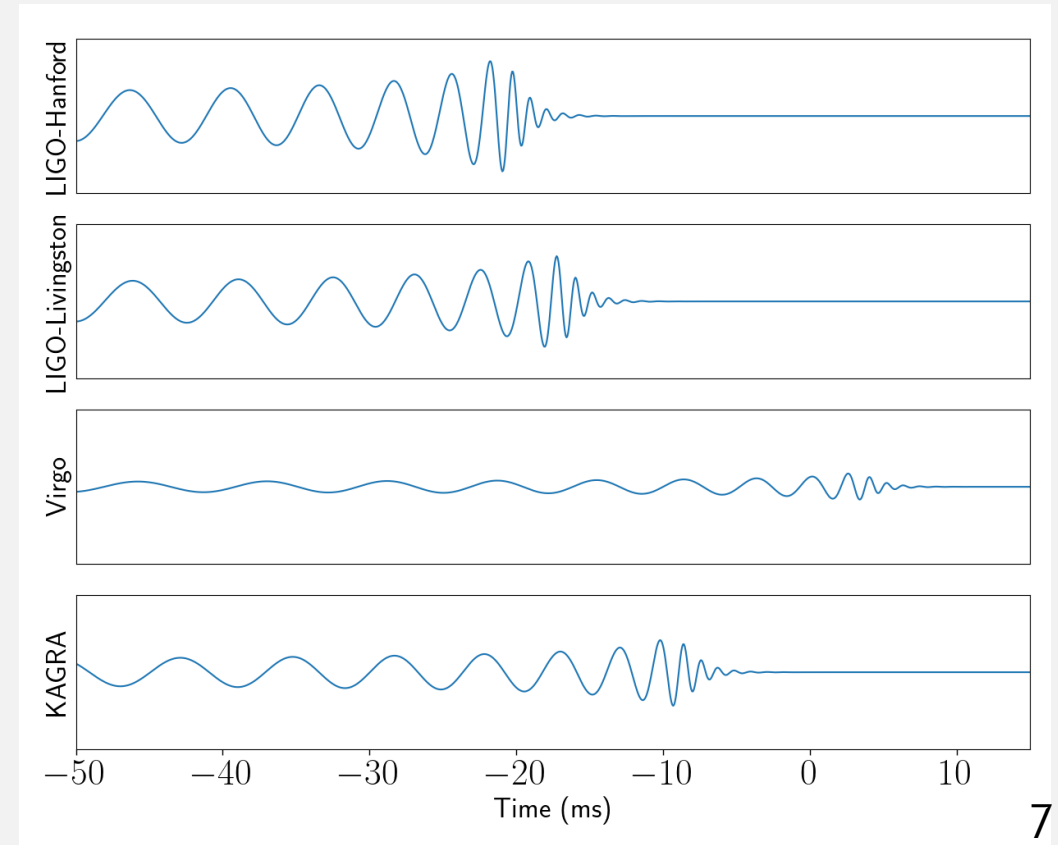


# Source direction

Gravitational waves



Source direction is estimated with arrival time, amplitudes, and phases observed at multiple detectors.



# Source parameters characterizing signal

**15** binary black hole parameters + **1** additional parameter **per neutron star**

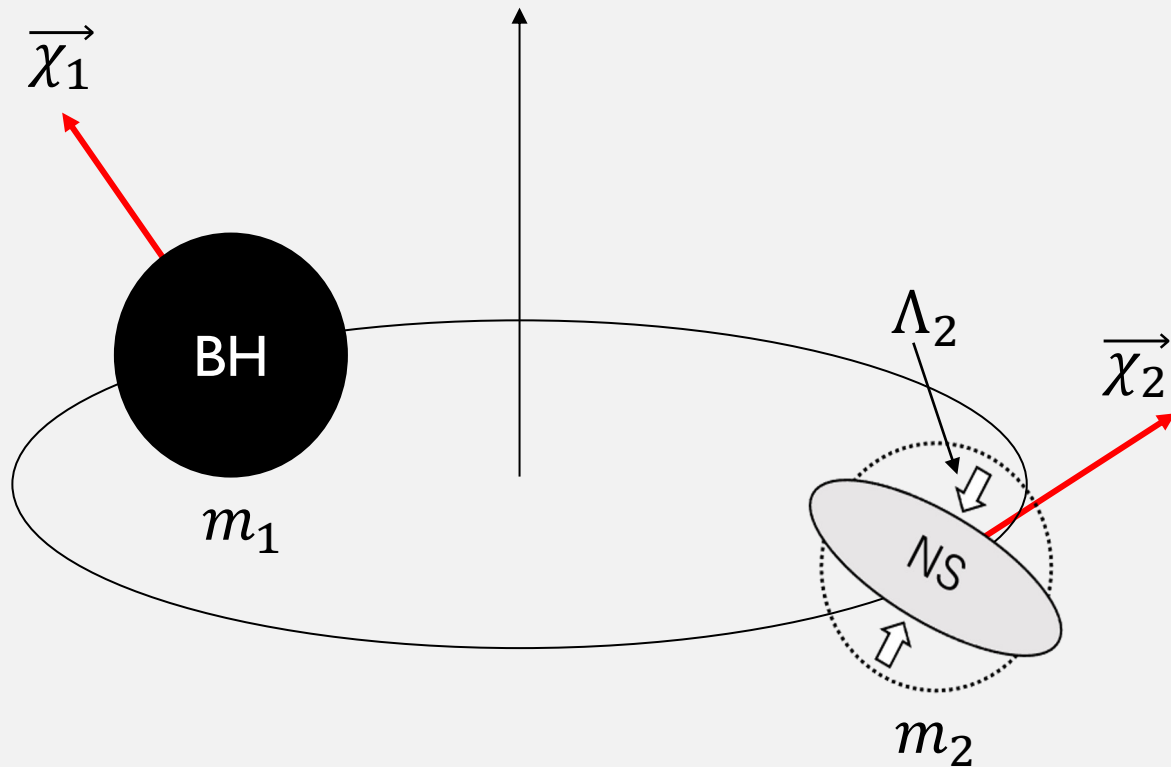


Figure: Schematic picture of neutron star black hole

- Masses:  $m_1, m_2$   
(Chirp mass  $\mathcal{M}$  and mass ratio  $q \equiv m_2/m_1$  used for efficiency)
- Spins:  $\vec{\chi}_1, \vec{\chi}_2$   
(Spin magnitudes and angles typically used)
- Tidal deformabilities:  $\Lambda_1, \Lambda_2$   
(only for neutron stars)
- Right ascension RA/declination Dec
- Coalescence time  $t_c$   
(Detector frame sky coordinates and time often used for efficiency)
- Luminosity distance  $D_L$
- Orbital inclination angle  $\theta_{JN}$
- Polarization angle  $\psi$
- Coalescence phase  $\phi_c$



# Calibration uncertainties

Due to uncertainties in detector calibration, observed signal can be slightly different from true signal:

$$\tilde{h}_{\text{observed}}(f) = \tilde{h}_{\text{true}}(f)(1 + \delta A(f))e^{i\delta\phi(f)}.$$

Additional  $2N_{\text{nodes}}$  parameters per detector:  
 $\{\delta A(f_i), \delta\phi(f_i)\}$  ( $i = 1, 2, \dots, N_{\text{nodes}}$ ).

L. Sun *et al.*, arXiv: 2107.00129.

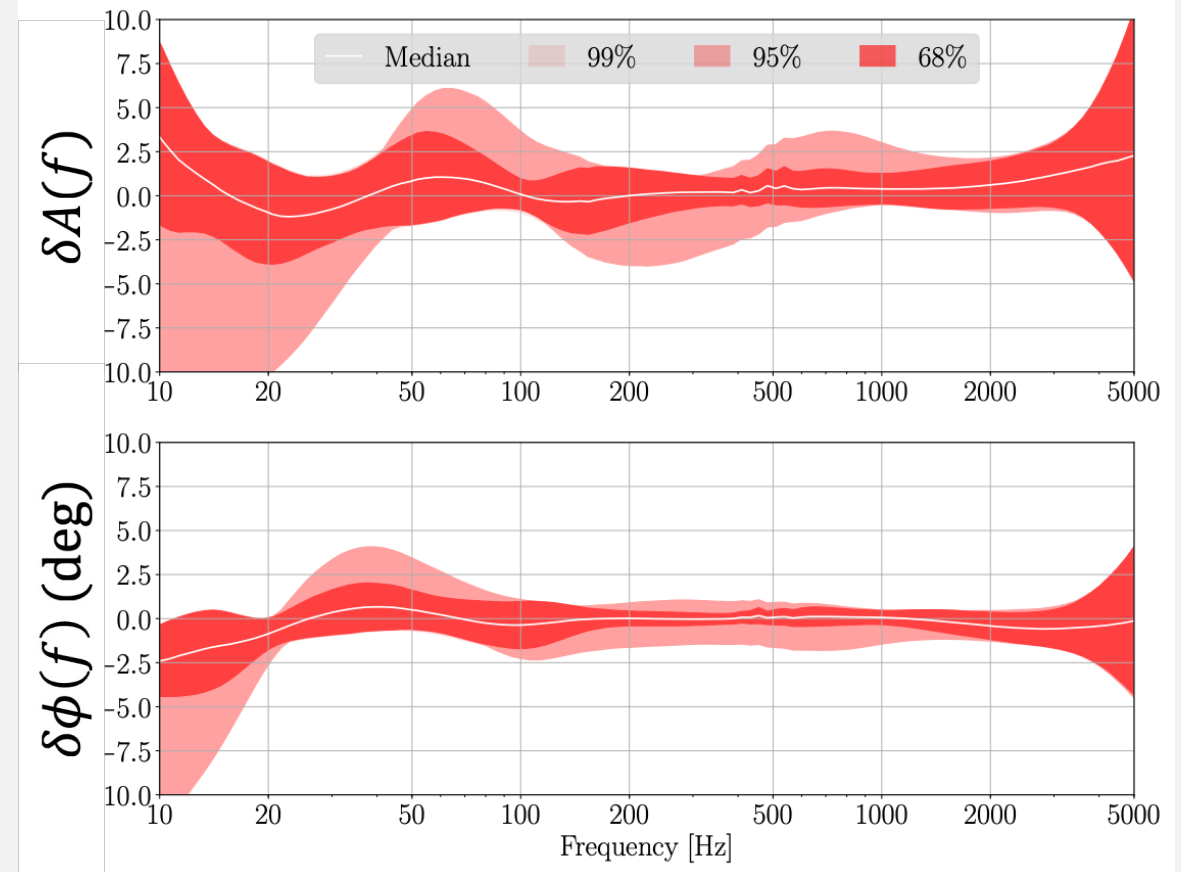


Figure: Calibration uncertainties of amplitude (top) and phase (bottom) of LIGO-Hanford in O3

# Bayesian inference

$$\text{Posterior} \rightarrow p(\theta | d, M) = \frac{\overset{\text{Likelihood}}{\downarrow} p(d | \theta, M) \overset{\text{Prior}}{\downarrow} p(\theta | M)}{p(d | M) \leftarrow \text{Evidence}}$$

$d$ : observed data

$\theta$ : parameters (masses, spins etc.)

$M$ : Signal hypothesis

# Bayesian inference

$$\text{Posterior} \rightarrow p(\theta | d, M) = \frac{\overset{\text{Likelihood}}{\downarrow} \mathcal{L}(d | \theta, M) \overset{\text{Prior}}{\downarrow} \pi(\theta | M)}{\mathcal{Z}(d | M) \leftarrow \text{Evidence}}$$

$d$ : observed data

$\theta$ : parameters (masses, spins etc.)

$M$ : Signal hypothesis

# Bayesian inference

$$\text{Posterior} \rightarrow p(\theta | d, M) = \frac{\overset{\text{Likelihood}}{\mathcal{L}(d | \theta, M)} \overset{\text{Prior}}{\pi(\theta | M)}}{\underset{\text{Evidence}}{\mathcal{Z}(d | M)}}$$

Prior encodes our **prior knowledge or belief on  $\theta$** .

- No information available  $\rightarrow$  Use uninformative prior (e.g. isotropic on RA/Dec, uniform in masses etc.).
- It can incorporate information from electromagnetic observations or astrophysics (e.g. fixed to RA/Dec from electromagnetic obs., astrophysical mass prior etc.).

# Bayesian inference

$$\text{Posterior} \rightarrow p(\theta | d, M) = \frac{\mathcal{L}(d | \theta, M) \pi(\theta | M)}{\mathcal{Z}(d | M)}$$

Likelihood                      Prior  
↓                                      ↓

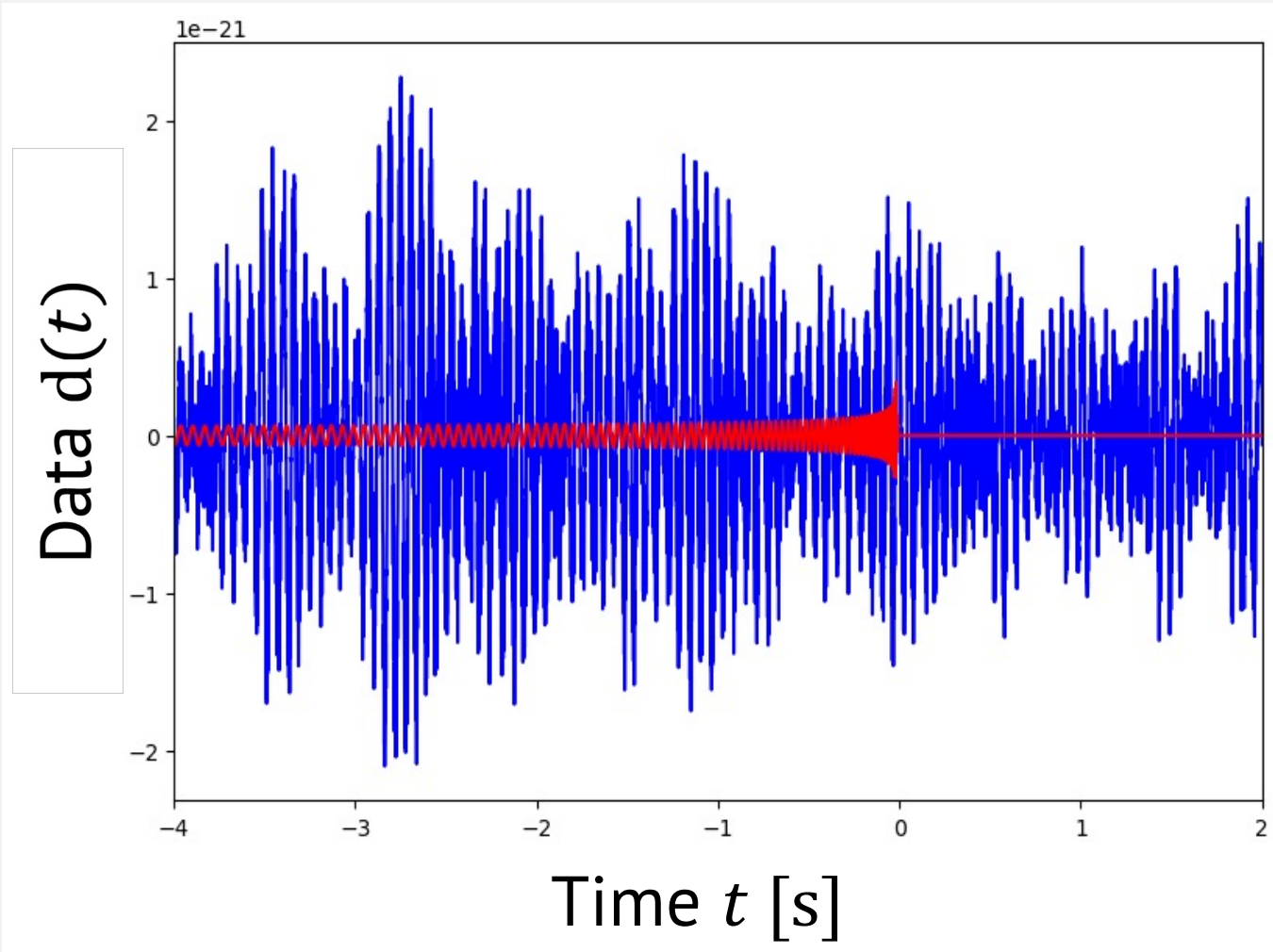
← Evidence

Evidence can be used for **comparing different hypotheses/models** (e.g. noise vs signal hypotheses, different waveform models etc.).

$$B = \frac{\mathcal{Z}(d | M_1)}{\mathcal{Z}(d | M_2)}, \quad B \gg 1 \rightarrow M_1 \text{ is favored}, \quad B \ll 1 \rightarrow M_2 \text{ is favored.}$$

$M_1, M_2$ : two different hypotheses/models

# Likelihood: $\mathcal{L}(d|\theta, M)$



**CBC signal**      **Noise**

$$d(t) = h(t; \theta) + n(t).$$

$$\mathcal{L}(d|\theta, M) = p(d - h(\theta) | \text{Noise})$$

## Likelihood: $\mathcal{L}(d|\theta, M)$

- Noise is **weakly stationary**:  $\langle n(t) \rangle = \text{const.}$ ,  $\langle n(t)n(t') \rangle = R(|t - t'|)$ .  
→  $\langle \tilde{n}(f_l) \rangle = 0$  ( $f_l = \frac{l}{T} > 0$ ,  $T$ : data duration),  $\langle \tilde{n}^*(f_l)\tilde{n}(f_{l'}) \rangle \simeq \frac{TS(f_l)}{2} \delta_{ll'}$ .

$S(f_l) = 2\langle |\tilde{n}(f_l)|^2 \rangle / T$  is referred to as **Power Spectral Density (PSD)** and characterizes noise variance at  $f_l$ .

- Noise follows **Gaussian distribution**.

## Likelihood: $\mathcal{L}(d|\theta, M)$

Those assumptions lead to **Whittle likelihood**,

$$p(n|\text{Noise}) = \exp\left(-\frac{2}{T} \sum_l \frac{|\tilde{n}(f_l)|^2}{S(f_l)}\right).$$

$$\longrightarrow \mathcal{L}(d|\theta, M) \propto \exp\left[-\frac{2}{T} \sum_l \frac{|\tilde{d}(f_l) - \tilde{h}(f_l; \theta)|^2}{S(f_l)}\right].$$

Higher likelihood  $\rightarrow$  Smaller residual  $|\tilde{d}(f_l) - \tilde{h}(f_l; \theta)|$

See J. Veitch et al. (2015): <https://arxiv.org/abs/1409.7215> for more context.



# PSD estimation

- Average tens-hundreds of data sets which do not contain signal:  
 $S(f_l) = 2\langle |\tilde{n}(f_l)|^2 \rangle / T$ .
- Fit the spectra of on-source data to mitigate biases from non-stationary noise (See Littenberg and Cornish (2015): <https://arxiv.org/abs/1410.3852>).

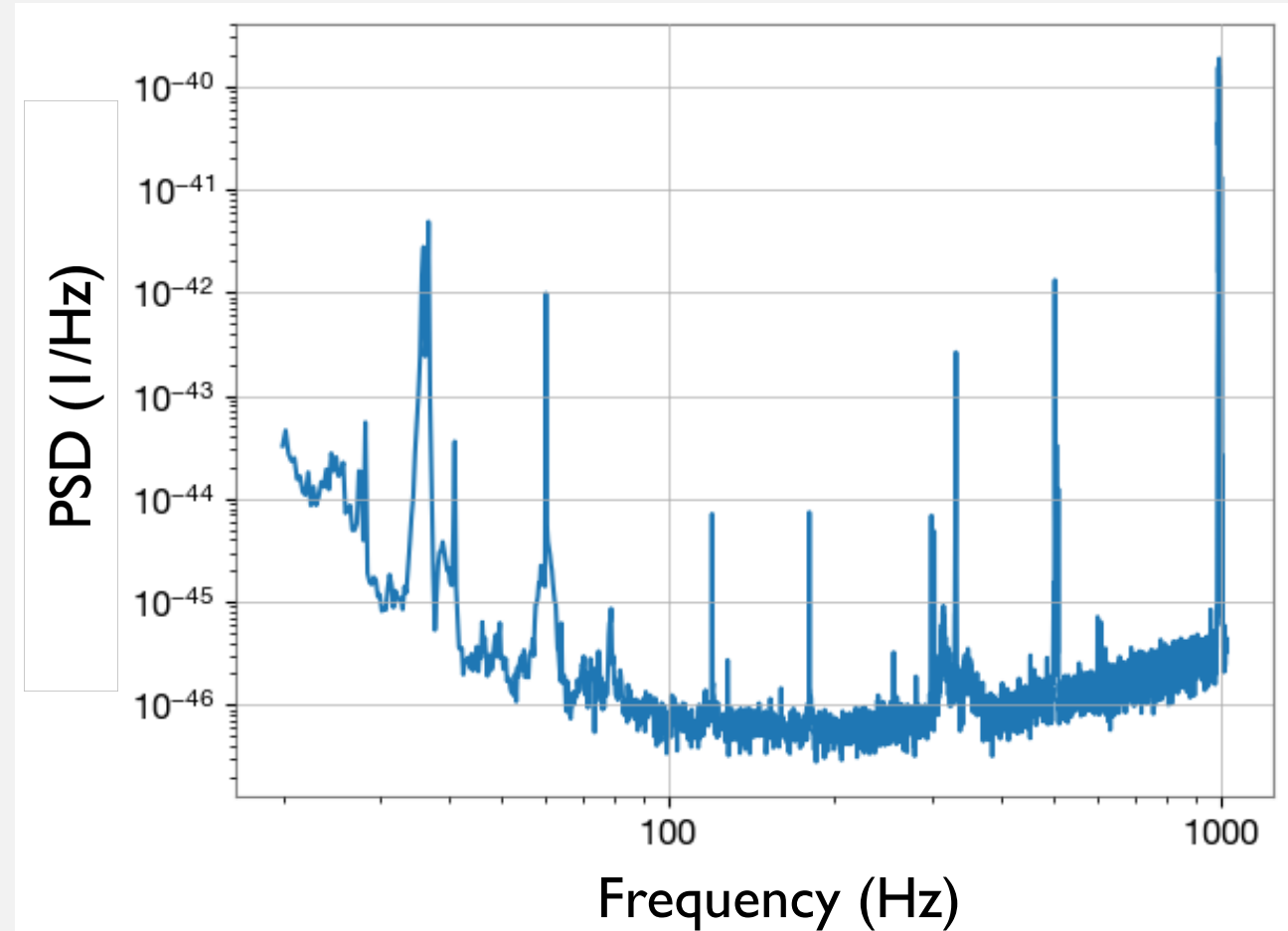


Figure: PSD estimated from data around GW150914

# Marginalization

- 1D posterior distribution

$$p(m_2|d, M) = \int p(\theta|d, M) \underbrace{dm_1 d\vec{\chi}_1 d\vec{\chi}_2 \dots}_{\text{Except for } m_2}$$

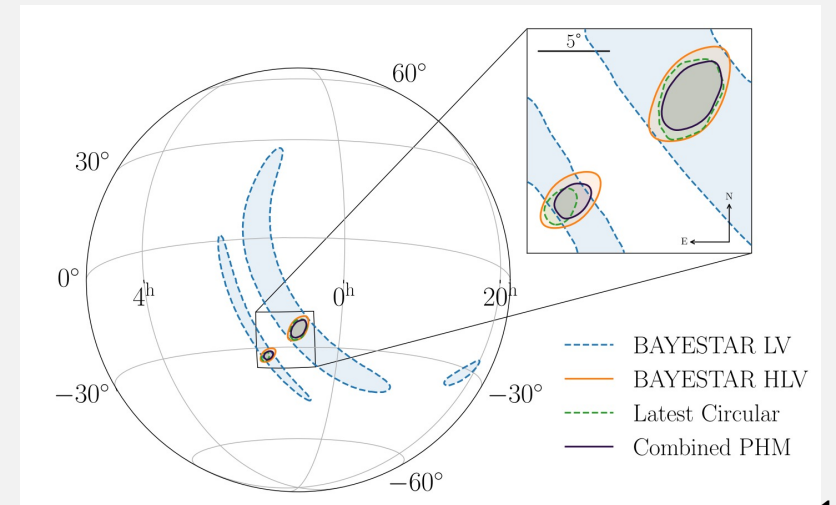
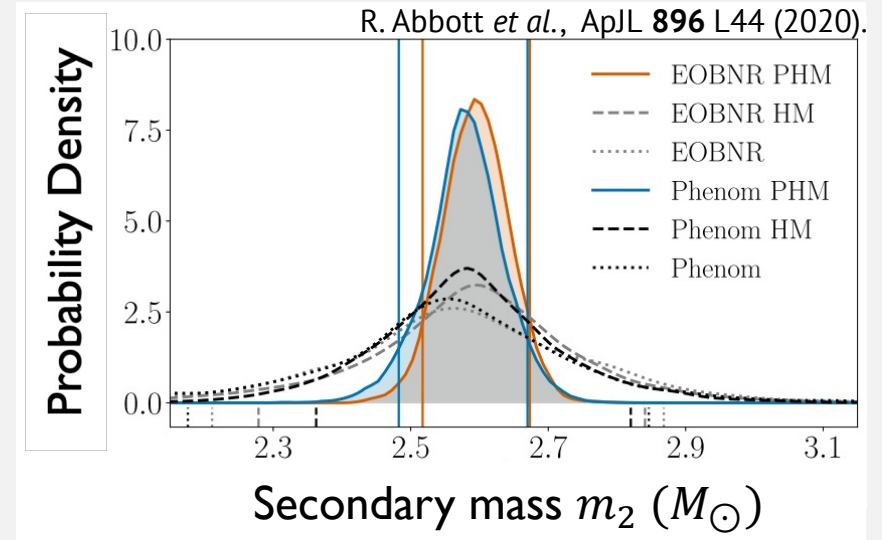
- 2D posterior distribution

$$p(\text{RA, Dec}|d, M) = \int p(\theta|d, M) \underbrace{dm_1 dm_2 d\vec{\chi}_1 d\vec{\chi}_2 \dots}_{\text{Except for RA, Dec}}$$

They require high-dimensional numerical integration.

Figure credit:

R. Abbott *et al.*, ApJL **896** L44 (2020).



Estimated source location of GW190814

# Stochastic sampling

Draw samples from posterior and histogram them!

Efficient algorithms for sampling

- Markov-chain Monte Carlo (MCMC)
- Nested sampling

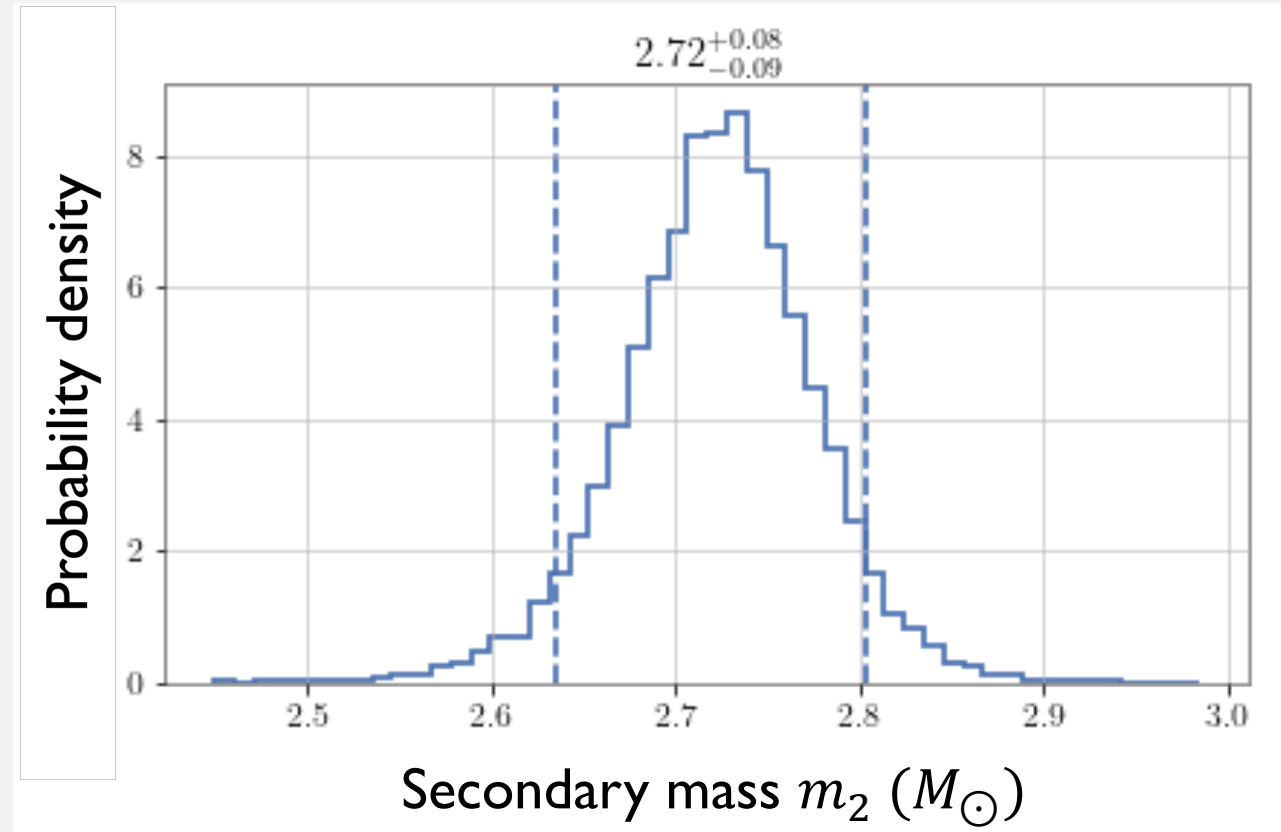
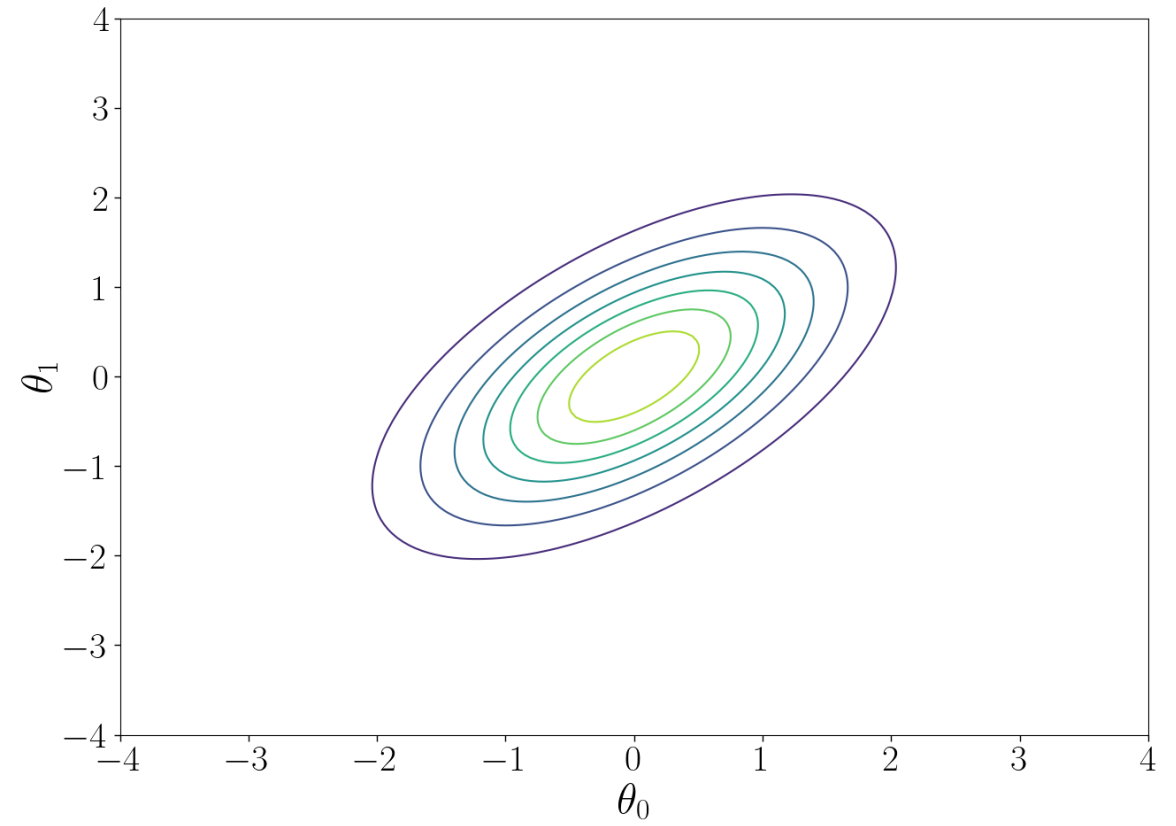


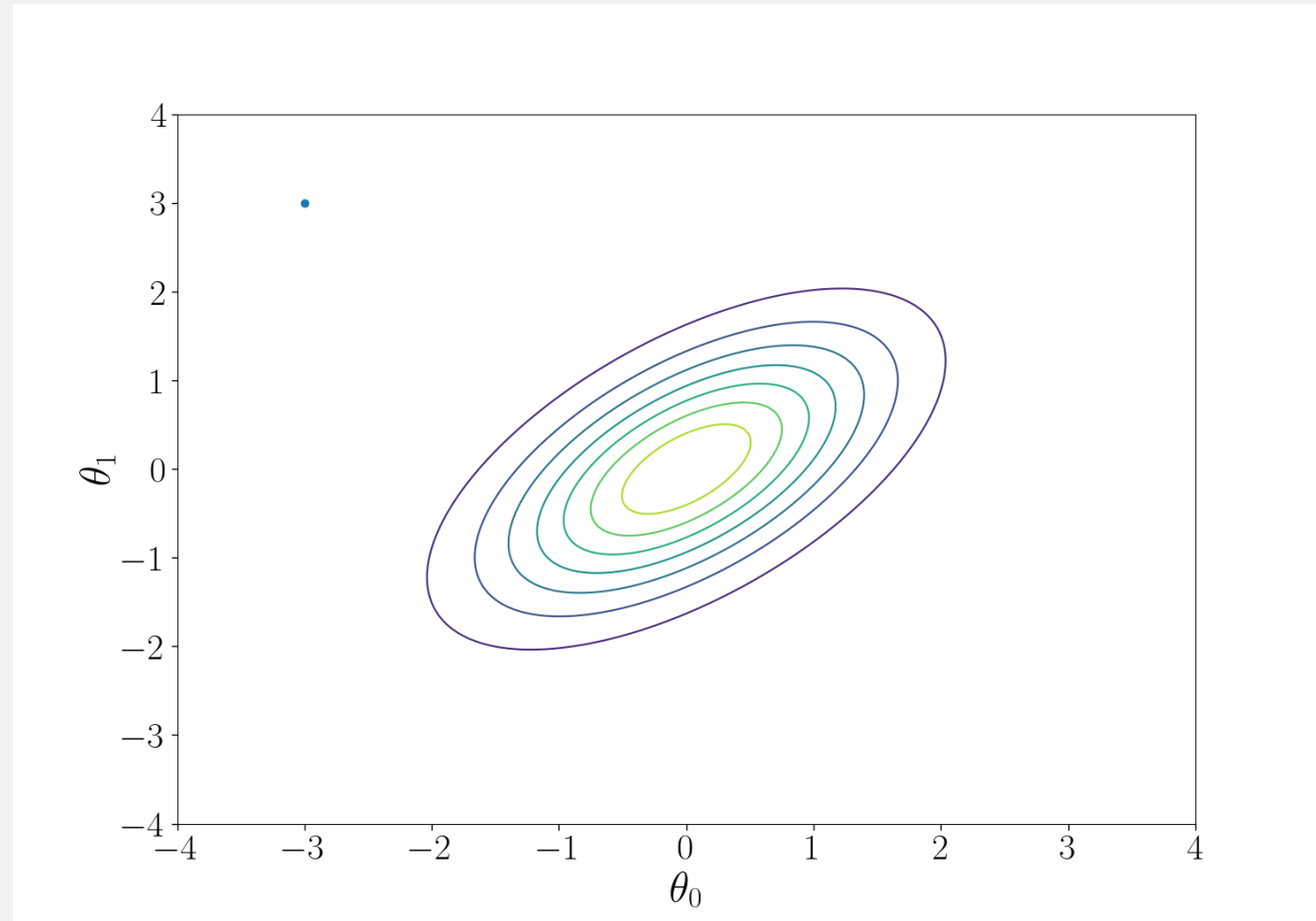
Figure: Estimated secondary mass of GW190814

# MCMC example: Metropolis-Hastings algorithm



# MCMC example: Metropolis-Hastings algorithm

Start from a random point  $\theta$ .



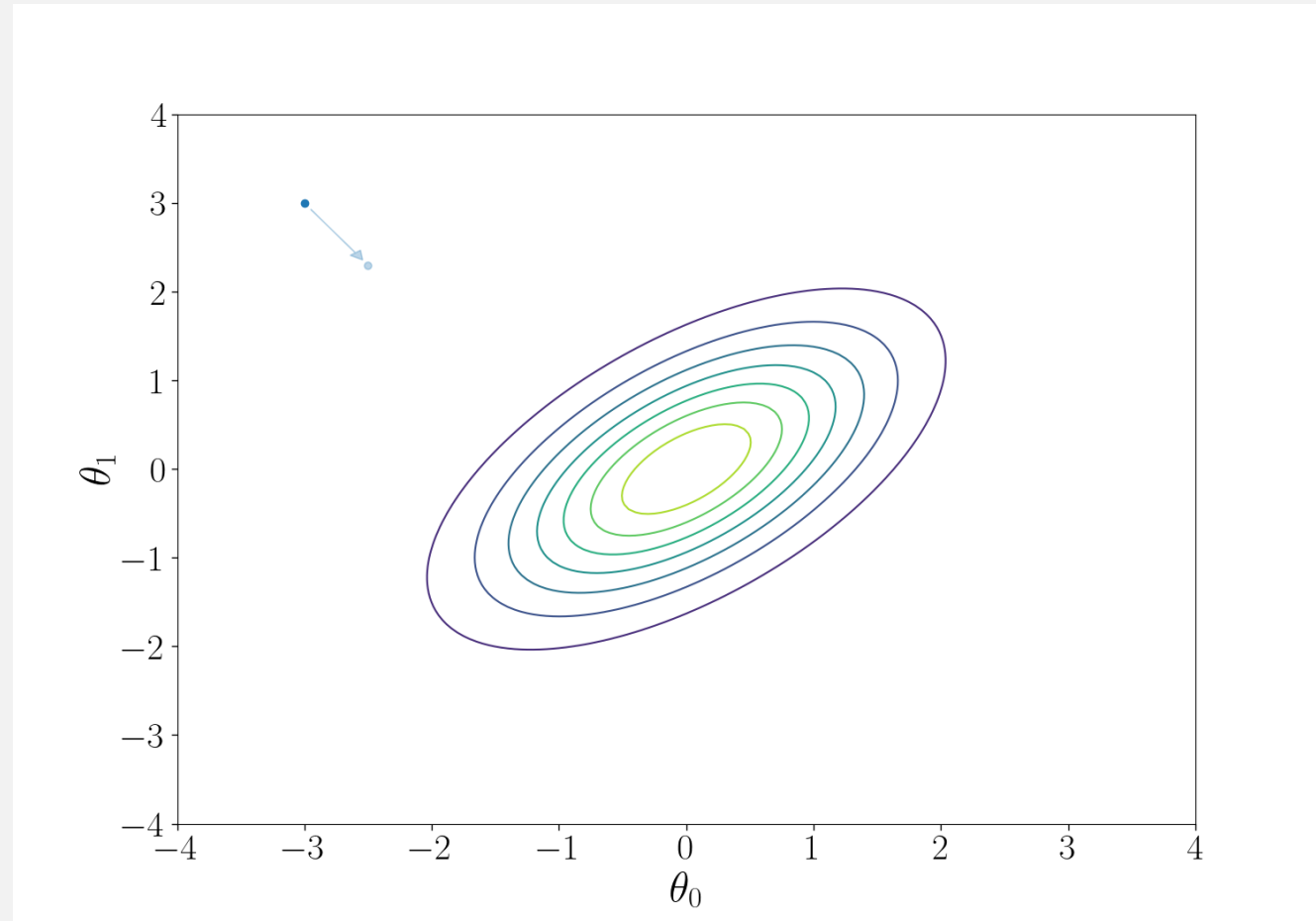
# MCMC example: Metropolis-Hastings algorithm

Start from a random point  $\theta$ .

Propose a next point  $\theta'$  with proposal distribution  $Q(\theta \rightarrow \theta')$ .

Accept that proposal with probability

$$\min \left\{ 1, \frac{p(\theta' | d, M) Q(\theta' \rightarrow \theta)}{p(\theta | d, M) Q(\theta \rightarrow \theta')} \right\}.$$

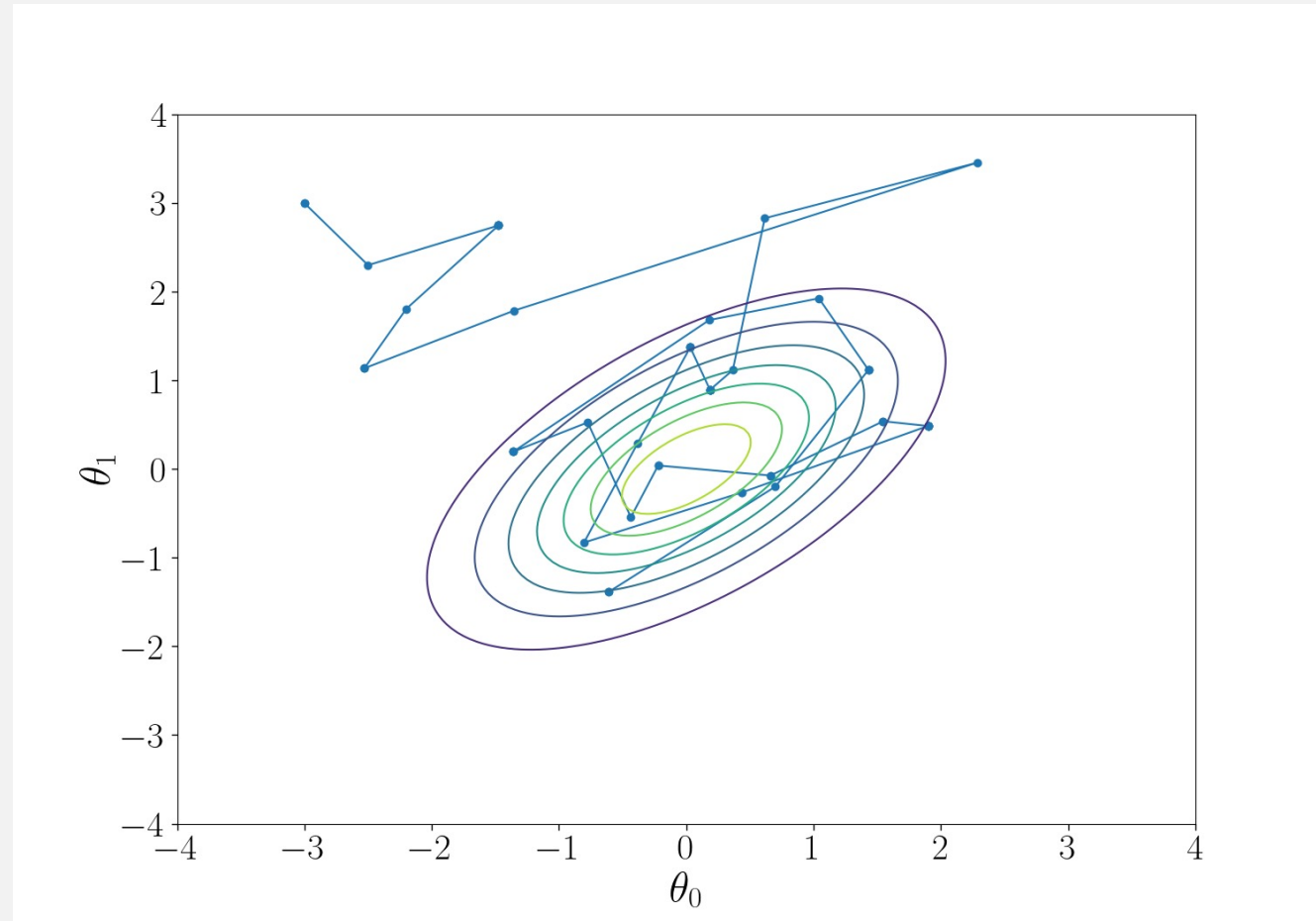


# MCMC example: Metropolis-Hastings algorithm

Start from a random point  $\theta$ .

Propose a next point  $\theta'$  with proposal distribution  $Q(\theta \rightarrow \theta')$ .  
Accept that proposal with probability  
of  $\min \left\{ 1, \frac{p(\theta'|d,M)Q(\theta' \rightarrow \theta)}{p(\theta|d,M)Q(\theta \rightarrow \theta')} \right\}$ .

Repeat this proposal-acceptance.



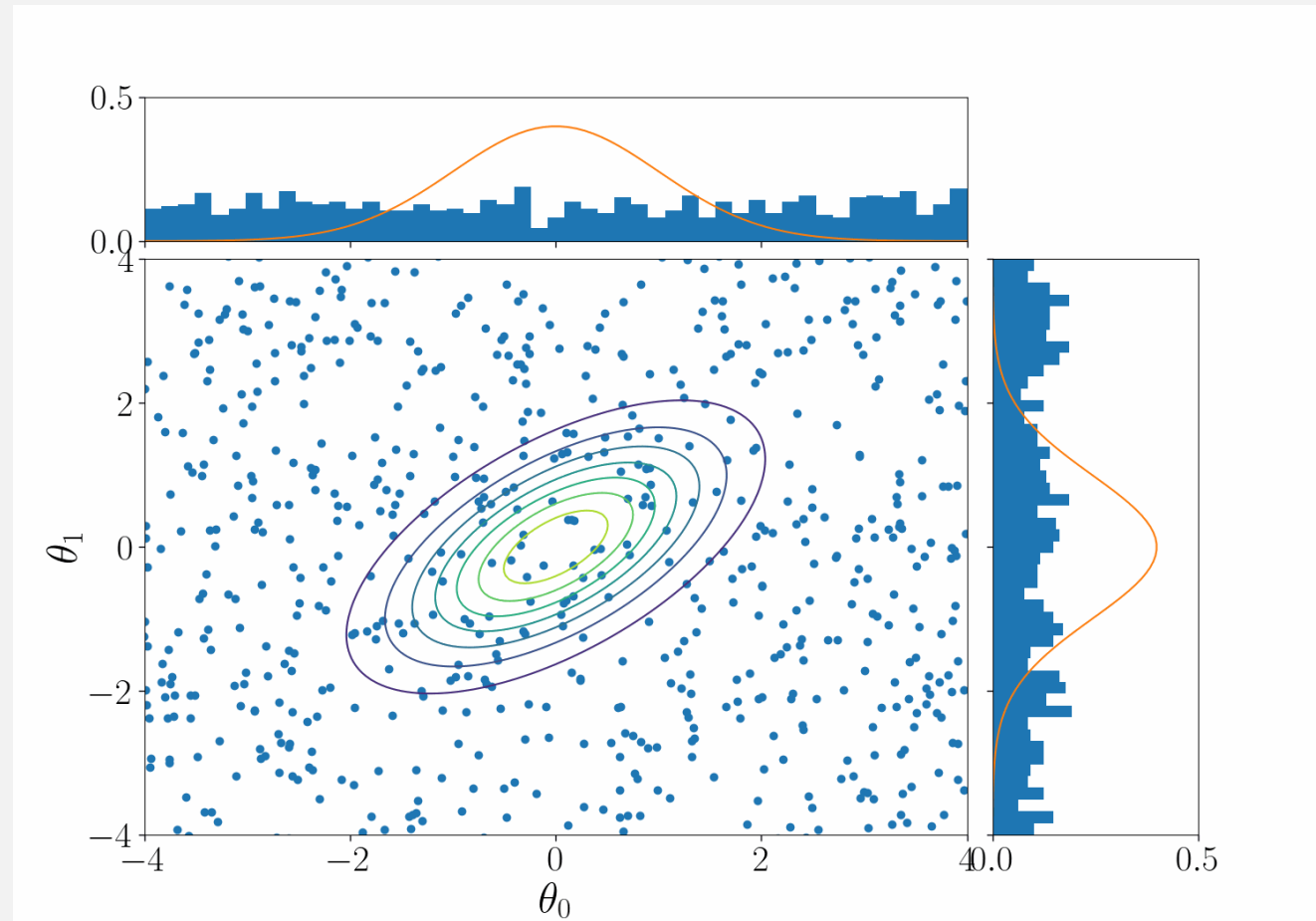
# MCMC example: Metropolis-Hastings algorithm

Start from a random point  $\theta$ .

Propose a next point  $\theta'$  with proposal distribution  $Q(\theta \rightarrow \theta')$ .  
Accept that proposal with probability of  $\min \left\{ 1, \frac{p(\theta'|d,M)Q(\theta \rightarrow \theta')}{p(\theta|d,M)Q(\theta' \rightarrow \theta)} \right\}$ .

Repeat this proposal-acceptance.

The random point **converges to a sample following posterior distribution.**





# Various open-source samplers

## MCMC sampler

- emcee:  
<https://emcee.readthedocs.io/>
- ptemcee:  
<https://github.com/willvousden/ptemcee>
- PyMC:  
<https://www.pymc.io/>
- zeus:  
<https://zeus-mcmc.readthedocs.io/>
- ....

## Nested samplers

- dynesty:  
<https://dynesty.readthedocs.io/en/latest/>
- nessai:  
<https://github.com/mj-will/nessai>
- Nestle:  
<http://kylebarbary.com/nestle/>
- pymultinest:  
<https://johannesbuchner.github.io/PyMultiNest/index.html>
- ....

# Bilby: a user-friendly Bayesian inference library

- Python codes, installable with pip/conda.
- All the components necessary for CBC parameter inference built in (likelihood, frequently-used priors, useful parameter conversion functions etc.)
- Supports open-source samplers and the native one: bilby-mcmc.
- Can be used for non-CBC problems (See Tutorial 3.1).
- Can simulate CBC signals as well as analyzing real data (See Tutorial 3.2).

References:

Ashton+ ApJS **241** 27 (2019),

Romero-Shaw+ MNRAS **499** 3 (2020).



# Playing with posterior samples

Posterior samples have been released from LVK.

- O1, O2:

<https://dcc.ligo.org/LIGO-P1800370/public>

- O3a:

<https://zenodo.org/record/6513631>

- O3b:

<https://zenodo.org/record/5546663>

In [2]: samples

Out[2]:

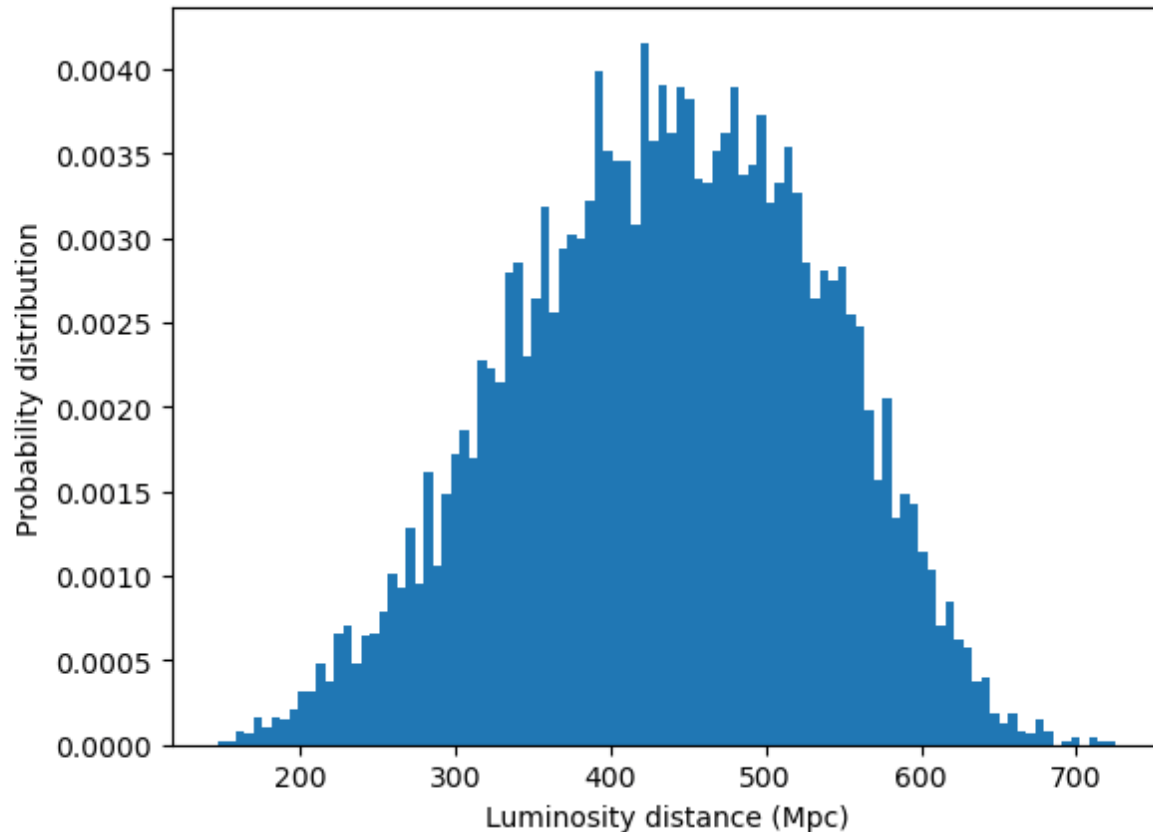
	costheta_jn	luminosity_distance_Mpc	right_ascension	declination	m1_detec
0	-0.976633	517.176717	1.456176	-1.257815	
1	-0.700404	401.626864	2.658802	-0.874661	
2	-0.840752	369.579071	1.106548	-1.136396	
3	-0.583657	386.935268	2.077180	-1.246351	
4	-0.928271	345.104345	0.993604	-1.069243	
...	...	...	...	...	...
8345	-0.691637	306.985025	1.485646	-1.269228	
8346	-0.834615	462.649414	2.065362	-1.265618	
8347	-0.911463	448.930876	1.536913	-1.257956	
8348	-0.856914	561.020036	2.367289	-1.211824	
8349	-0.919556	519.641782	1.916675	-1.250801	

8350 rows x 10 columns

# Playing with posterior samples

```
In [3]: import matplotlib.pyplot as plt

plt.hist(samples["luminosity_distance_Mpc"], density=True, bins=100)
plt.xlabel("Luminosity distance (Mpc)")
plt.ylabel("Probability distribution")
plt.show()
```



Histogram of samples gives  
**1D posterior distribution.**

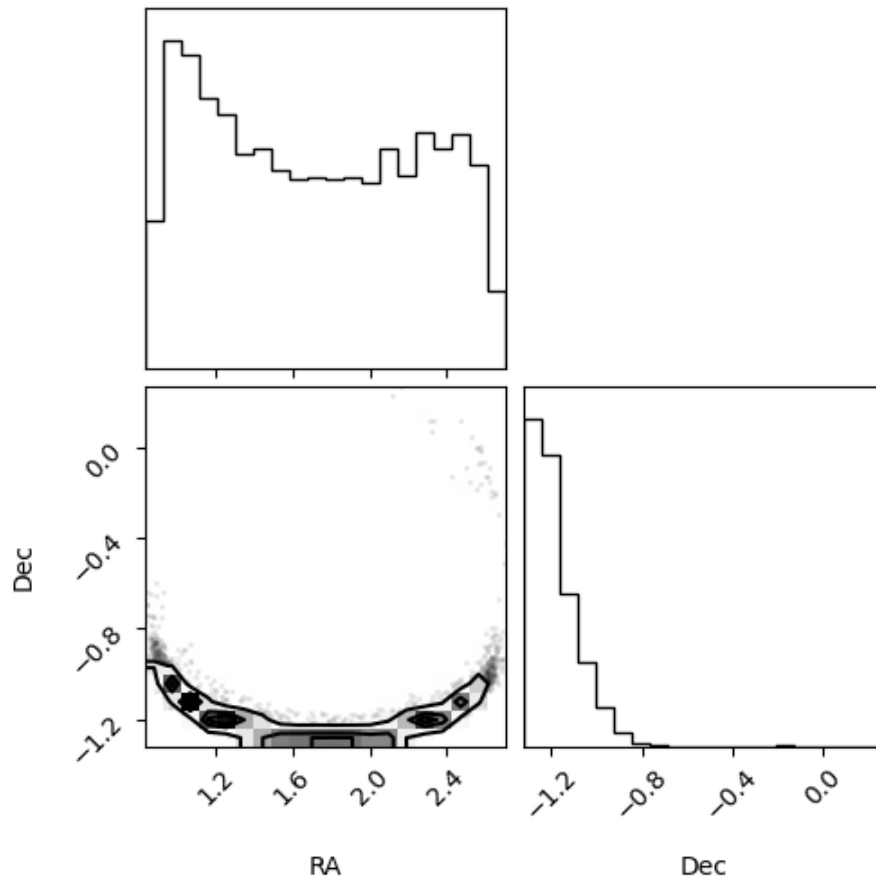
**The 90% credible interval**  
can be obtained by  
calculating the 5th and  
95th percentiles of samples.

# Playing with posterior samples

```
In [11]: import corner
import numpy as np

corner.corner(
    np.array([samples["right_ascension"], samples["declination"]]).T,
    labels=["RA", "Dec"]
)
```

Out[11]:



2D histogram is useful to understand correlation.

See Tutorial 3.3 to learn more about reading/plotting samples.

# Conclusion

- Source parameters such as **masses, spins, and tidal deformability parameters of colliding objects** can be measured with observed gravitational-wave waveform.
- Source parameter estimation is typically performed with **Bayesian inference**, where likelihood is computed under the assumption of **stationary Gaussian noise**.
- We **generate random samples** following Bayesian posterior probability distribution and **make their histograms** to estimate source parameter values we are interested in.
- Useful references
  - Bilby documentation: <https://lscsoft.docs.ligo.org/bilby/>
  - Thrane and Talbot (2019): <https://arxiv.org/abs/1809.02293>

# Tests of general relativity (GR)

Introduce parameters controlling deviation from GR predictions:

$$\tilde{h}(f) = A(f)e^{i\Phi(t)}, \quad \Phi(t) = \Phi_{GR}(t) + \Delta\varphi_n f^{\frac{n-5}{3}}.$$

Credit: B. P. Abbott et al., PRL **123**, 011102 (2019).

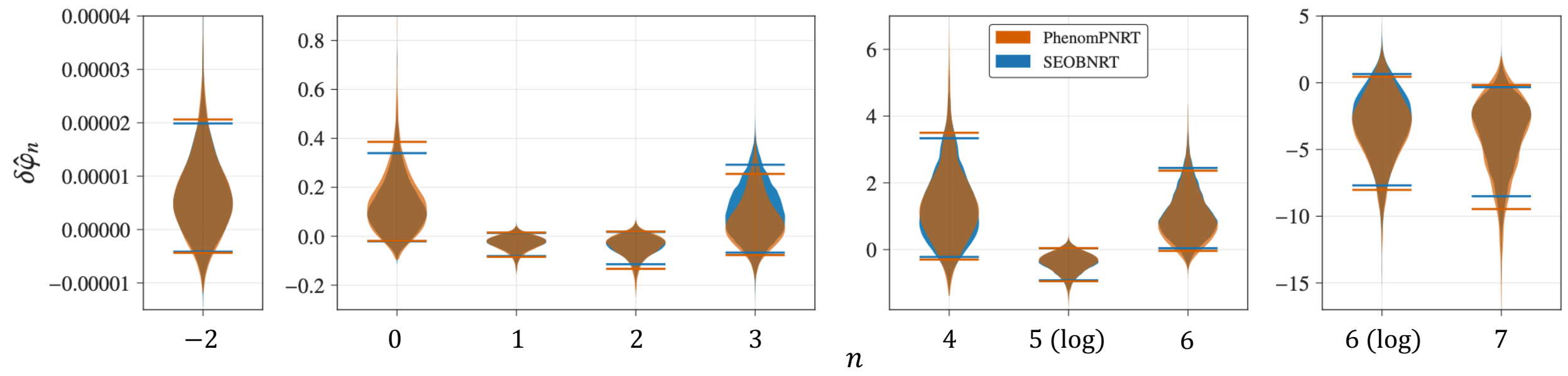


Figure: Constraints on deviation of GW170817 from GR predictions